Morphology of GPS and DPS-TEC over an equatorial station: validation of IRI and NeQuick 2 models.

Olumide O. Odeyemi[1], Jacob Adeniyi[2], Olushola Oladipo[3], Olayinka Olawepo[3], Isaac Adimula[3], Elijah Oyeyemi[1]
[1] Department of Physics, University of Lagos, Nigeria.
[2] Department of Physical Sciences, Landmark University, Omu-Aran, Nigeria.
[3] Department of Physics, University of Ilorin, Nigeria.

Correspondence to: Olumide O. Odeyemi (oodeyemi@unilag.edu.ng; adeniyi.jacob@lmu.ng.edu)

0.0 Abstract

We investigated total electron content (TEC) at Ilorin (8.50^{o}N 4.65E, dip lat. 2.95) for the year 2010, a year of low solar activity in 2010 with R_z=15.8. The investigation involved the use of TEC derived from GPS, estimated TEC from digisonde portable sounder data (DPS), the International Reference Ionosphere (IRI) and NeQuick 2 (NeQ) models. During the sunrise period, we found that the rate of increase in DPS-TEC, IRI-TEC, and NeQ-TEC was higher with compared with GPS-TEC. One reason for this can be alluded to an overestimation of plasmaspheric electron content (PEC) contribution in modeled TEC and DPS-TEC. A correction factor around the sunrise, where our finding showed a significant percentage deviation between the modeled TEC and GPS-TEC, will correct the differences. Our finding revealed that during the daytime when PEC contribution is known to be absent or insignificant, GPS-TEC and DPS-TEC in April, September, and December predict TEC very well. The lowest discrepancies were observed in May, June, and July (June solstice) between the observed and all the model values at all hours. There is an overestimation in DPS-TEC that could be due to extrapolation error while integrating from the peak electron density of F2 (NmF2) to around ~ 1000 km in the Ne profile. The underestimation observed in NeQ-TEC must have come from the inadequate representation of contribution from PEC on the topside of the NeQ model profile, whereas the exaggeration of PEC contribution in IRI-TEC amount to overestimation in GPS-TEC. The excess bite-out observed in DPS-TEC, and modeled-TEC shows the indication of over-prediction of fountain effect in these models. Therefore, the daytime bite-out observed in these models requires a modifier that could moderate the perceived fountain effect morphology in the models accordingly. The daytime DPS-TEC performs better than the daytime IRI-TEC and NeQ-TEC in all the months. However, the dusk period requires attention due to highest percentage deviation recorded especially for the models in March, November, and December. Seasonally, we found

that all the TECs maximize and minimize during the March equinox and June solstice, respectively. Therefore, GPS-TEC and modeled TEC reveal the semi-annual variations in TEC.

Keywords: (Total Electron Content (TEC); International Reference Ionosphere (IRI) and NeQuick 2 Models)

1.0 Introduction

Total electron content (TEC) is the total number of free electrons in a columnar of one square meter along the radio path from the satellite to the receiver on the Earth. TEC exhibits diurnal, seasonal, solar cycle and geographical variations. Therefore, the physical and dynamical morphology of the TEC over a given location is of great importance in trans-ionospheric communications during both quiet and disturbed geomagnetic conditions (Jesus et al., 2016; Tariku, 2015; Akala et al., 2012; Aravindan and Iyer, 1990 and Olawepo et al., 2015). GPS-TEC is quantified from the GPS orbiting satellites to the GPS receiver station on the Earth, with an approximate distance of 20200 km (Liu et al., 2006). Thus, a typical GPS-TEC measurement incorporates the complete plasmaspheric electron content (PEC). The digisonde portable sounder (DPS) estimates the bottomside and topside TEC to obtain the total TEC from the electron density (Ne) profile. The topside DPS-TEC is extrapolated from the peak electron density of the F2 region (NmF2) to around ~ 1000 km thus, the significant PEC contribution from the higher altitudes is omitted from DPS-TEC measurement (Belehaki et al., 2004; Zhang et al., 2006 and Reinisch and Huang, 2001).

The International Reference Ionosphere (IRI) model depends on worldwide data from various measurements (Bilitza, 2001; Bilitza, 1986; Bilitza and Rawer, 1998). The IRI model provides reliable ionospheric densities, composition, temperatures, and composition in the ionospheric altitude range (Bilitza, 2001; Radicella et al., 1998 and Coisson et al., 2009). The latest version of the IRI model can be found at all time on the web (http:nssdc.gsfc.nasa.gov/space/model/ions/iri.html) with improvements on earlier versions of the model. The NeQuick 2 (NeQ) models makes use of the position, time and solar flux or sunspot number over a given location are variables in the NeQ model code (Coisson et al., 2006; Andreeva and Lokota, 2013 and Bidaine and Warnant, 2011). The output of the NeQ program and corresponding TEC are by the electron density along any ray-path and numerical integration in space and time respectively.

The availability of ionospheric parameters for global ionospheric models is deficient over the African sector compared to the consistent input of the data from the Asian and American sectors. Therefore, the continuing investigations of the parameters over Africa are required to improve the global ionospheric model. For example, Bagiya et al. (2009) studied TEC around equatorial-low latitude region at Rajkot (22.29° N, 70.74° E, dip 14.03° N) during low solar activity, Olwendo et al. (2012) and Karia and Pathak (2011) investigated the TEC data at Kenyan and Surat (India), respectively. They all noticed a semi-annual variation with minimum and maximum TEC in June solstice and March equinox, respectively. Using Faraday rotational technique, Olatunji (1967) investigated TEC variation over the equatorial latitude at Ibadan. He observed no daytime bite-out and seasonal anomaly over the region. Rastogi et al. (1975) observed the diurnal variation of TEC using Faraday rotation over the magnetic equator. They noticed that TEC at the topside was higher than TEC at the bottomside during the nighttime, however during the daytime; they observed a uniform distribution of the TEC, on the topside and the bottomside of Ne profile.

Regarding the DPS-TEC measurement, Barbas et al. (2010) examined GPS-TEC and DPS-TEC at Tucuman (26.69◦S, 65.23◦W) during different seasons. They inferred that the DPS-TEC represented the GPS-TEC with a minimal discrepancy in all seasons. Reinisch et al. (2004) investigated GPS-TEC and DPS-TEC at mid-latitude and equatorial region. They observed that the variations of GPS-TEC and DPS-TEC appeared similar, but the daytime values of GPS-TEC were higher than daytime DPS-TEC. Zhang et al. (2004) studied the variations of DPS-TEC and GPS-TEC over Hainan and reported that the daytime DPS-TEC and GPS-TEC were close in values during the daytime, but during the dusk period, they observed a significant discrepancy between DPS-TEC and GPS-TEC. Belehaki et al. (2004) extracted the plasmaspheric electron content (PEC) from the GPS-TEC at Athens (38°N, 23.5°E) for over a year. They reported a maximum and minimum contribution of PEC in the morning and evening, respectively. Mosert et al. (2007), Jodogne et al. (2004) and Mckinnell et al. (2007) concluded that approximated PEC from the GPS-TEC and DPS-TEC is possible in colocated GPS and DPS station. Adewale et al. (2012), Okoh et al. (2015), Jee and Scherliess (2005), Kenpankho et al (2013), Sulungu et al. (2017), and Migoya Orué et al. (2008) validated the IRI-TEC with GPS-TEC at different regions

and found high discrepancies between the IRI-TEC and GPS-TEC when compared different IRI-model options.

Concerning NeQ model, Cherniak and Zakharenkova (2016) validated NeQ model. They established underestimation of the topside ionosphere above ~ 500km in the NeQ model, due to inaccurate representation of topside Ne profile. Rabiu et al. (2014) validated NeQ model using GPS-TEC over the equatorial region of Africa. They reported that the upper boundary of NeQ model, up to 20,000 km needed to be adjusted to accommodate the PEC-TEC in NeQ model. Leong et al. (2013) investigated TEC and NeQ models. They found that the observed and NeQ TEC were close in values during dusk periods, but the changed TEC revealed higher discrepancies during the post-sunset. Yu et al. (2012) investigated the monthly average of NeQ-TEC model over three stations in China (Changchun, Beijing, and Chongqing) during the quietest period. They revealed that NeQ correctly predicted GPS-TEC. However, the NeQ-TEC underestimated the GPS-TEC during the dusk period. Rios et al. (2007) investigated the variations of DPS-TEC and IRI-TEC and found that DPS-TEC was smaller compared to IRI TEC. McNamara (1985) observed discrepancies between DPS-TEC and IRI-TEC and found that the IRI underestimated the DPS-TEC during the daytime. Obrou et al. (2008) compared the DPS-TEC and IRI-TEC at Korhogo during high and low solar activity. They found that the variations of DPS-TEC and IRI-TEC were close in values during high solar activity (HSA) and low solar activity (LSA), but the performance of IRI-TEC was better during HSA compared to LSA.

The current contributions of Africa on the improvement of ionospheric models (IRI and NeQuick) are not adequate compared with the continuous support received from Asia and South America. The insufficient instrumentation at the equatorial region of Africa has a considerable effect on the shortcoming. Therefore, the constant validation of IRI and models with the observed parameter is necessary for an improved ionospheric model. Furthermore, the investigation on DPS-TEC has not been reported extensively for comparison purpose over the equatorial region of Africa. Therefore, this study investigates the linked morphologies between the variations of GPS-TEC and DPS-TEC, and validations of IRI-TEC, and NeQ-TEC models with the observed parameters. Our finding will inform the suitability of modeled TEC in place of GPS-TEC. The result will also determine the appropriate model for the equatorial latitude in

Africa. Thus, the deviations in TEC obtained from the combined relationship between GPS-TEC, DPS-TEC, IRI-TEC, and NeQ-TEC could be used to correct the discrepancy in the models.

2.0 Methods of Analysis of GPS and DPS Data

Data used for this study are those of the five quietest days of each month of the year 2010. The five quietest days are days (with Ap $\leq$ 4) for which geomagnetic activities are quiet, the are obtained from the international quiet days (IQD) table available on the website of Australia Geosciences. The data are for Ilorin (8.50^{o}N 4.65E, dip lat. 2.95) during the year 2010, a year of low solar activity. TEC data were obtained with GPS receiver and Digisonde Portable Sounder (DPS) both of which are located at the Ionospheric Laboratory of the University of Ilorin. The methods of data processing are described in the sections below.

2.1 GPS-TEC

The slant TEC records from GPS have errors due to satellite differential delay (satellite bias (bs)) and receiver differential delay (receiver bias (br)) and receiver inter-channel bias (b_{SR}). This uncorrected slant GPS-TEC measured at every one-minute interval from the GPS receiver derived from all the visible satellites at the Ilorin station are converted to vertical GPS-TEC using the relation below in equation (1).

$$(\mathrm{GPS-TEC})_V = (\mathrm{GPS-TEC})_S - [b_S + b_R + b_{SR}]/S(E) \quad (1)$$

Where $(\mathrm{GPS-TEC})_S$ is the uncorrected slant GPS-TEC measured by the receiver, S(E) is the obliquity factor with zenith angle (z) at the Ionospheric Pierce Point (IPP), E is the elevation angle of the satellites in degrees and $(\mathrm{GPS-TEC})_V$ is the vertical GPS-TEC at the IPP. The equation two below provides S(E) as

$$S(E) = \frac{1}{\cos(z)} = \left[1 - \left(\frac{R_E \times \cos(E)}{R_E + h_s}\right)^2\right]^{-1/2} \quad (2)$$

Where R_E is the mean radius of the Earth measured in kilometer (km), and h_S is the height of the ionosphere from the surface of the Earth, which is approximately equal to 400 km according to Langley et al. (2002) Rama Rao et al., (2006a) and Mannucci et al. (1993) . The five quietest

slant GPS-TEC data for each month in the year 2010 were interpreted using Krishna software (Global positioning system total electron content analysis application user's manual, 2009, Institute for Scientific Research, Boston College, Chestnut Hill, Massachusetts). This software reads raw data and corrects all source of errors mentioned above from Global Navigation Satellite System service (IGS) code file. A minimum elevation angle of 20 degrees is used to avoid multipath errors. The estimated vertical GPS-TEC data is a function of a two sigma (2σ) iteration. This sigma is a measure of GPS point positioning accuracy. We converted the average one-minute VTEC data to hourly averages.

2.2 DPS-TEC

Regarding the total electron content (TEC) from the digisonde portable sounder (DPS), the Standard Archive Output (SAO) files obtained from the DPS at the University of Ilorin were edited to remove magnetically disturbed days. Huang and Reinisch (2001) technique was used to compute the DPS-TEC. The vertical DPS-TEC computation by the technique is based on the application of the integration over the vertical electron density [Ne(h)] profile as shown in the equation (3) below.

$$\mathrm{TEC} = \int_0^{\mathrm{hmF\,2}} \mathrm{Ne_B}(\mathrm{dh}) + \int_{\mathrm{hmF\,2}}^{1000} \mathrm{Ne_T}\,(\mathrm{dh}) \qquad 3$$

Where $\mathrm{Ne_B}$ and $\mathrm{Ne_T}$ are the bottomside and topside Ne profiles, respectively. We computed the NeB from the recorded ionograms by using the inversion technique developed by Huang and Reinisch (1996). The information above the peak of the F2 layer is absent from the record of the ionogram. Thus, the $\mathrm{Ne_T}$ is measured by approximating the exponential functions with suitable scale height (Bent et al., 1972) with a less estimated error of 5%. The ionograms were manually scaled and inverted into electron density profile using the NHPC software and later processed with the SAO explorer software based on the technique described above to obtain the TEC (Reinisch et al., 2005). We estimated an average of TEC for each hour over the selected days. The universal time (UT) is the time standard for the record of GPS and DPS data, but we converted UT to local time (LT) by adding one hour to corresponding UT. Nigeria is 1 hour in advance of Greenwich Mean Time (GMT) thus, 0100 UT is the same as 0200 LT in Ilorin, Nigeria. The available months of the year were grouped into seasons in order to study the seasonal variation of TEC and the performances of some of the options in the IRI model..The four seasons are grouped as March equinox or MEQU (March, and April), June solstice or

JSOL (June, and July), September equinox or SEQU (September, and October) and December solstice or DSOL (November, December). The monthly median of the five quietest days were deduced and the average of the monthly median under a particular season as defined above to infer seasonal variations under GPS-TEC, DPS-TEC, IRI-TEC, and NeQ-TEC. The DPS in Ilorin was installed in March, 2010, as a result data were not available for the months of January to late March, 2010. Therefore, this study does not include the days for which DPS data were not available.

2.3 Validation of IRI - 2016 and NeQuick 2 Models

We correlated the observed TEC with modeled TEC in the IRI-2016 model. The website http://www.ccmc.gssfc.nasa.gov/modelweb/models/iri_vitmo.php provides the modeled TEC values. We selected the upper boundary height 2000 km and the B0 table option for the bottomside shape parameter. The equations 3a, 3b, and 3c represent the difference between GPS-TEC and DPS-TEC, GPS-TEC and IRI-TEC and GPS-TEC and NeQ-TEC while equations 4a, 4b, and 4c below show the percentage change between GPS-TEC and DPS-TEC, GPS-TEC and IRI-TEC, and GPS-TEC and NeQ-TEC.

$$\Delta_{\mathrm{DPS-GPS}} = \mathrm{DPS_{TEC}} - \mathrm{GPS_{TEC}} \quad (3a)$$

$$\Delta_{\mathrm{IRI-GPS}} = \mathrm{IRI_{TEC}} - \mathrm{GPS_{TEC}} \quad (3b)$$

$$\Delta_{\mathrm{NeQ-GPS}} = \mathrm{NeQ_{TEC}} - \mathrm{GPS_{TEC}} \quad (3c)$$

$$\%(\Delta_{\mathrm{DPS-GPS}}) = \frac{\mathrm{DPS_{TEC}} - \mathrm{GPS_{TEC}}}{\mathrm{DPS_{TEC}}} \times 100 \quad (4a)$$

$$\%(\Delta_{\mathrm{IRI-GPS}}) = \frac{\mathrm{IRI_{TEC}} - \mathrm{GPS_{TEC}}}{\mathrm{IRI_{TEC}}} \times 100 \quad (4b)$$

$$\%\left(\Delta_{\mathrm{NeQ-GPS}}\right) = \frac{\mathrm{NeQ_{TEC}} - \mathrm{GPS_{TEC}}}{\mathrm{NeQ_{TEC}}} \times 100 \quad (4c)$$

$\Delta_{\mathrm{DPS-GPS}}$, $\Delta_{\mathrm{IRI-GPS}}$, and $\Delta_{\mathrm{NeQ-GPS}}$ represent the difference between GPS-TEC and DPS-TEC, GPS-TEC and IRI-TEC, and GPS-TEC and NeQ-TEC, respectively while $\%(\Delta_{\mathrm{DPS-GPS}})$, $\%(\Delta_{\mathrm{IRI-GPS}})$, and $\%\left(\Delta_{\mathrm{NeQ-GPS}}\right)$, represent the percentage deviation between GPS-TEC and DPS-TEC, GPS-TEC and IRI-TEC, and GPS-TEC and NeQ-TEC, respectively.

The Abdus Salam International Centre for Theoretical Physics (ICTP) - Trieste, Italy in collaboration with the Institute for Geophysics, Astrophysics and Meteorology (IGAM) of the

University of Graz, Austria developed the web front-end of NeQuick. This quick-run ionospheric electron density model developed at the Aeronomy and Radiopropagation Laboratory modeled TEC along any ground-to-satellite straight line ray-path. Therefore, we validated the NeQ obtained from https://t-ict4d.ictp.it/nequick2/nequick-2-web-model.

3.0 Result

3.1 Monthly Median Variations of GPS and modeled TEC

Figure 1a shows the simultaneous plots of hourly variations of the monthly median of TEC obtained from GPS-, DPS-, IRI-, and NeQ- TEC during the quiet period. The GPS-TEC is in black line with the star symbol; the DPS-TEC is in green line with the diamond symbol, IRI-TEC is in red line with zero symbols, and finally, the NeQ-TEC is in blue line with multiplication symbol. All the TEC plots are regulated by the same local time (LT) on the horizontal axis. The result reveals that the morphologies of GPS-, DPS-, modeled-TEC increase gradually from the sunrise period (0700 - 0900 LT) and reach the daytime maximum, mostly around (1200 - 1700 LT), and then later decay steadily until a minimum value around 0600 LT. Therefore, our result suggests that the diurnal variations of the observed and modeled TEC capture the well known solar zenith angle dependence of TEC since both observed and modeled TEC characterize pre-sunrise minimum, daytime maximum, daytime depression (modeled TEC) and post-sunset decay. The lowest and highest pre-sunrise minimum ranged from ~ 0.66 TECU (DPS) - ~ 4.49 TECU (DPS) while the lowest and highest daytime maximum found between ~ 17.75 TECU (NeQ) - ~ 38.0 TECU (DPS). The result shows noontime bite-out in modeled TEC around 1200 LT and 1500 LT except in GPS-TEC where the bite-out was obscure except that a slight shift in daytime maximum within 1500 and 1700 LT in all months. We observed two moderate peaks (pre-noon and post-noon peaks) in DPS-TEC and modeled TEC indicating the bite-out effect on the modeled and DPS- TEC signatures. We also found around the sunrise period, the model TEC rises faster than the GPS-TEC, but IRI-TEC rises faster compared to DPS-TEC and IRI-TEC. Between 0600 and 0900 LT, the lowest and highest difference in the rises of IRI-TEC compared to GPS-TEC were ~ 5.0 TECU (March) and ~ 15.3 TECU (November), respectively. The post noontime decay was faster in DPS-TEC compared to GPS-TEC and modeled TEC in all months. Figure 1b reveals the coincident seasonal variations of GPS-; DPS-; and modeled-TEC during a quiet period of (i) March Equinox, (ii) June solstice,

(iii) September equinox and (iv) December solstice. The daytime maximum ranges are between ~ 24.8 TECU (NeQ) - ~ 34 TECU (DPS), ~ 19.2 TECU (NeQ) - ~ 22.6 TECU (DPS), ~ 24.9 TECU (NeQ) - ~ 33.5 TECU (DPS) and ~ 24.55 TECU (NeQ) - ~ 31 TECU (DPS), in March equinox, June solstice, September equinox, and December solstice, respectively. We observed that the morphologies of GPS-TEC and modeled TEC maximize and minimize at March equinox and June solstice, thus indicating semi-annual variation in observed and modeled TEC.

3.2 Percentage deviation of DPS-TEC; IRI-TEC; and NeQ-TEC

Figures 2(a), 3(a), and 4(a), are hourly variations of deviation in TEC (ΔTEC) between GPS, DPS, IRI and NeQ derived TEC whereas Figures 2(b), 3(b), and 4(b) depict the mass plots of hourly variations in the percentage deviation (% ΔTEC) during a quiet period from March - December. In Figure 2a and 2b, the overestimation by DPS-TEC as given by $\Delta TEC_{DPS-GPS}$ is within the range of ~ 5.13 TECU (March) - ~ 19.12 TECU (July) around 0700 - 1600 LT while the underestimation $\Delta TEC_{DPS-GPS}$ fluctuated between ~ 3.2 TECU (June) - ~ 16.4 TECU (November) around 1700 - 2400 LT. The overestimation and underestimation of $\%\Delta_{IRI-GPS}$ ranged from ~ 2% - ~ 49% and ~ - 1.36% - ~ - 306%, respectively. From Figures 3a and 3b, the overestimation occurred regularly around 0400 - 1200 LT in all months. The overestimated and underestimated $\Delta TEC_{IRI-GPS}$ were between ~ 9.13 TECU (July) - ~ 15.3 TECU (November) and ~ 0.15 TECU (October) - ~ 0.95 TECU (July), respectively. However, a few underestimation and overestimation of $\Delta TEC_{IRI-GPS}$ still occurred irregularly around 1300 - 0300 LT in all months. The result also shows that IRI-TEC completely overestimated GPS-TEC in May and June within 0100 and 2400 LT. The overestimation of $\%\Delta TEC_{IRI-GPS}$ ranged between ~ 0.1% to ~ 86% in all months. In Figures 4a and 4b, NeQ-TEC overestimated GPS-TEC within 0100 - 1100 LT and 2000 - 2400 LT with $\Delta TEC_{NeQ-GPS}$ ranged from ~ 9.72 (September) and ~ 0.01 (April). We also found that NeQ-TEC underestimated $\Delta TEC_{NeQ-GPS}$ was between ~ 9.72 (Nov) - ~ 0.11(May). The overestimation and underestimation of $\%\Delta TEC_{NeQ-GPS}$ are within ~ 0.02% - ~ 81% and ~ - 0.3% - ~ - 75% respectively.

3.3 Comparisons of the percentage deviations from GPS-TEC

From Figure 2b, 3b, and 4b, the percentage deviation between GPS- and DPS-TEC are more significant; greater than 100% in March-August, September, November, and December

between 0400 - 0500 LT and around 2200 - 2400 LT in June and July. The percentage deviation between GPS- and IRI-TEC are also lower than 100% except in March around 0400 LT whereas the difference between GPS- and IRI-TEC is greater than 100%. The percentage deviations in DPS and modeled-TEC during dusk periods are always higher than their corresponding deviations during the daytime. During the daytime, the deviations are smaller in DPS and NeQ-TEC compared to IRI-TEC.

4.0 Discussion of Result

An investigation into the variations of GPS-TEC, DPS-TEC, and the validations of modeled-TECs at an equatorial region (8.50N 4.650 E) in Africa during low solar activity in the year 2010 has been carried out. The TEC increases gradually from the sunrise period, then slowly reaches the daytime maximum, and later decays to the pre-sunrise minimum. This result indicates that the observed and modeled-TEC are a solar zenith angle dependence showing peak and least TEC values during the noontime and dusk time, respectively (Wu et al.2008; Aravindan and Iyer 1990; and Kumar and Singh 2009). Interestingly, our result that reveals the faster rise in the DPS-TEC compared to GPS-TEC during sunrise is not consistent with the findings of Ezquer et al. (1992) at Tucumán (26.9° S; 65.4° W), Belehaki et al. (2004) at Athens, McNamara (1985) at low latitude and Obrou et al. (2008) at Korhogo (9.33°N, 5.43°W, Dip = 0.67°S). They all found that the GPS-TEC increased faster than the DPS-TEC during the sunrise. The enrichment of plasmaspheric electron content (PEC) on TEC latterly reported by Belehaki et al. (2004) indicated a significant PEC increase in the morning and dusk time. Recently, Jodogne et al. (2004), Mosert et al. (2007), and Mckinnell et al. (2007) also obtained a rough estimation of PEC from the GPS and DPS-TEC variations. They inferred that the combined GPS-TEC and DPS-TEC could give the PEC contribution in TEC of a given location. Therefore, the higher rise in DPS-TEC compared to GPS-TEC during the sunrise in our study could be attributed to inaccurate representation of PEC in the topside DPS-TEC profile while extrapolation from the peak of F2 region (NmF2) to around ~ 1000 km of the Ne profile. Therefore, a typical TEC measurement naturally includes a meaningful PEC contribution (Belehaki et al. 2003; Balan and Iyer, 1983; Carlson, 1996; and Breed et al., 1997).

306 The higher values in DPS-TEC compared with IRI-TEC around sunrise is not consistent
307 with Rios et al. (2007) who investigated the comparison of DPS-TEC and IRI-TEC. They found
308 that DPS-TEC is smaller than IRI-TEC at all hours. They assumed that the prediction of IRI-
309 TEC had included the high topside Ne profile. Thus, our observation may suggest that the IRI-
310 TEC has incorporated low topside Ne profile in the IRI model or the excessive enhancement of
311 PEC contribution in the topside Ne profile in the DPS-TEC.
312
313 The closeness observed during daytime between GPS-TEC and DPS-TEC in April,
314 August and December may also suggest that the topside Ne profile in GPS-TEC is accurate in
315 the DPS-TEC topside profile due to the absence of or negligible PEC contribution in DPS-TEC
316 values. The insignificant daytime PEC observed in this study is consistent with Rastogi et al.
317 (1971) and Belehaki et al. (2004). Higher daytime DPS-TEC compared with daytime IRI-TEC
318 is consistent with the result of McNamara (1985). However, Obrou et al. (2008) at the equatorial
319 latitude, found higher IRI-TEC relative to DPS-TEC at the low solar activity. Therefore, the
320 reduced daytime IRI-TEC compared to GPS-TEC values indicates the excessive PEC removal
321 from the model values that its PEC contribution had been raised initially during the sunrise.
322 Also, the reduced NeQ-TEC compared to GPS-TEC values in all months is consistent with the
323 report of Migoya-Orue et al. (2017), Zakharenkova (2016), Rabiu et al., (2014) and Nava and
324 Radicella (2009). They recommended an added PEC contribution on topside NeQ profile for an
325 accurate prediction of NeQ model.
326
327 The daytime bite-out in TEC is due to the occurrence of the most active fountain effect
328 during the noontime at the magnetic equator. The bite-out results from the vertical plasma drift
329 due to the combined consequence of mutually perpendicular electric and magnetic fields on the
330 plasma. The drift lifts the plasma at the magnetic equator and diffuses along geomagnetic field
331 lines into the high latitudes, therefore, leaving the reduced TEC at the magnetic equator
332 (Bandyopadhyay, 1970; Olwendo et al., 2013; Skinner, 1966; Bolaji et al., 2012). However, the
333 absence of daytime bite-out (Olatunji, 1967) in GPS-TEC in our finding may be due to the more
334 great productions at the bottomside and topside electron content that are enhanced quickly to
335 replenish the loss of the ionization that occurs through the fountain effect during the noontime.
336

The percentage difference between observed and modeled-TEC reveal that the pre-sunrise values in DPS-TEC, IRI-TEC, and NeQ-TEC require modifications especially during the month of March for DPS-TEC and the models, and November and December for DPS-TEC only. The daytime DPS-TEC is closer to the GPS-TEC value compared to the daytime IRI-TEC and NeQ-TEC values. The nighttime NeQ-TEC and IRI-TEC perform better with GPS-TEC compared with DPS-TEC in all months. There is also the need to minimize the discrepancies observed during the dusk periods.

Seasonally, we found that TEC maximizes and minimizes during the equinoxes and the solstices, respectively. Our report is consistent with Mala et al. (2009), Wu et al. (2008), Kumar and Singh (2009), and Balan and Rao, (1984) who investigated TEC in various regions. They attributed the seasonal variation in TEC to the seasonal differences in thermospheric composition. Moreover, the sub-solar point is around the equator during the equinox. Consequently, the sun shines directly over the equatorial latitude, and in addition to the high ratio of O/N2 around the region, this translates to stronger ionization, and generates a semi-annual variation in TEC. The finding from our study is consistent with the reports of Ross Skinner, (1966), Bolaji et al. (2012), and Scherliess and Fejer (1999) who obtained semi-annual variation in TEC. Scherliess and Fejer (1999) also concluded that daytime E × B drift velocity could result in semi-annual variation because the drift is more and less significant in the equinoctial months and June solstice, respectively.

5.0 Conclusion

We have examined the variations of observed and modeled TEC over an equatorial region in Africa during a year of low solar activity. Our findings showed that:

(i) GPS-TEC and modeled TEC are solar zenith angle dependence.

(ii) a faster sunrise increase in the modeled TEC relative to GPS-TEC which suggest a overestimation of the topside Ne profile of the modeled TEC due to plasmaspheric electron content (PEC) into the models.

(iii) a good representation of the daytime measured TEC by the and models, suggesting that the model TEC could represent GPS-TEC in the absence of plasmaspheric TEC contribution.

(iv) the $\Delta TEC_{IRI-GPS}$ and % $\Delta TEC_{IRI-GPS}$ in May and June consistently show overestimations within 0100 - 2400 LT indicating the enhanced contribution of PEC at all hours in May and June.

(v) the percentage deviations in DPS and modeled-TEC relative to GPS-TEC during dusk periods is always higher than their corresponding differences during the daytime, and the values of daytime deviation in DPS and NeQ-TEC are smaller compared to daytime deviation in IRI-TEC. This study was carried out during a low solar activity in the year 2010; it will be of advantage to investigate and compare similar reviews during high solar activity with our results.

6.0 Acknowledgments

The authors thank the US Air Force and Lowell Digisonde, Massachusetts for the donation and continual maintenance of the DPS. We also appreciate Boston College and the SCINDA group for the donations and continual maintenance of the GPS receiver at the University of Ilorin, Nigeria. We also appreciate the support of the University of Ilorin and CAR-NASRDA for their support in funding of the Ionospheric observatories.

7.0 References

Adewale, A.O., Oyeyemi, E.O., and Olwendo, J. (2012): Solar activity dependence of total electron content derived from GPS observations over Mbarara. Advances in Space Research. **50,** 415– 426.

Akala, A.O., E O Oyeyemi, E O Somoye, A B Adeloye, and A.O., Adewale. 2010. Variability of foF2 in the African Equatorial Ionosphere. Advances in Space Research 45 (11). COSPAR: 1311–14. doi:10.1016/j.asr.2010.01.003.

Andreeva, E. S., and M. V Lokota. 2013. Analysis of the Parameters of the Upper Atmosphere and Ionosphere Based on Radio Occultation, Ionosonde Measurements, IRI and NeQuick Model Data. 52(10):1820–26. doi.org/10.1016/j.asr.2013.08.012.

Aravindan, P., and Iyer, K. N. (1990): Day-to-day variability in ionospheric electron content at low latitudes, Pmet. Space Sci., **38**(6),743-750.

Bagiya, Mala S, H.P Joshi, K N Iyer, M Aggarwal, S Ravindran, and B M Pathan. 2009. "TEC Variations during Low Solar Activity Period (2005-2007) near the Equatorial Ionospheric Anomaly Crest Region in India." Annales Geophysicae 27: 1047–57. doi:10.5194/angeo-27-1047-2009.

Balan, N., and Rao, P. B. (1984): Relationship Between Nighttime Total Electron Content Enhancements, Journal of Geophysical Research, **89(**10), 9009-9013.

Balan, N., Iyer, K.N. Equatorial anomaly in ionospheric electron content and its relation to dynamo currents. J. Geophys. Res. 88 (A12), 10259– 10262, 1983.

Bandyopadhyay, P. (1970): Measurement of total electron content at Huancayo, Peru, Planet. Space Sci., **18**, 129–135, doi:10.1016/0032-0633 (70)90150-9.

Barbas, Haro B. De, C. Medina, and V. H. Rios. 2010. "differences between GPS and digisonde measurements of total electron content." 45(4):403–16.

Belehaki, A Jankowski, N.Reinisch B. W. 2004. "Plasmaspheric Electron Content Derived from

GPS TEC and Digisonde Ionograms." 33:833–37.
Belehaki, A., and Kersley, L. (2003): Statistical validation of the ITEC parameter, Third Workshop of the COST271 Action, 23-27 September 2003, Spetses, Greece.
Bent, R.B., Llewellyn, S.K. and Schmid, P.E., 1972. A highly successful empirical model for the worldwide ionospheric electron density profile. DBA Systems, Melbourne, Florida.
Bidaine, B. and R. Warnant. 2011. "Ionosphere Modelling for Galileo Single Frequency Users : Illustration of the Combination of the NeQuick Model and GNSS Data Ingestion." Advances in Space Research 47(2):312–22. doi.org/10.1016/j.asr.2010.09.001).
Bilitza, D. (2001): 'International Reference Ionosphere 2000', Radio Science, **36(**2), 261-275.
Bilitza, D. (1986): International reference ionosphere: Recent developments, Radio Science, **21**, 343-346.
Bilitza, D., and Rawer, K. (1998): "International Reference Ionosphere Model (IRI- 93," http://envnet.gsfc.nasa.gov/Models/EnviroNET-Models.html Adv. Space Res., **69**, 520–829.
Bolaji, O. S., Adeniyi, J. O., Radicella, S. M., and Doherty, P. H. (2012): Variability of total electron content over an equatorial West African station during low solar activity. Radio Science, **47**, RS1001 doi:10.1029/2011RS004812.
Breed, A.M, G L Goodwin, A-m Vandenberg, E A Essex, K J W Lynn, and Abstract Ionospheric. 1997. Ionospheric Total Electron Content and Slab Thickness J . H . Silby 32 (4): 1635–43. 10.1029/97RS00454 2006.
Carlson, H.C. Incoherent scatter radar mapping of polar electrodynamics. J. Atmos. Solar-Terr. Phys. 58 (1–4), 37–56, 1996.
Cherniak, I., and Zakharenkova, I. (2016). NeQuick and IRI-Plas model performance on topside electron content representation: Spaceborne GPS measurements. *Radio Science*, *51*(6), 752-766.
Coïsson, P., Radicella, S.M., Leitinger, R. and Nava, B., 2006. Topside electron density in IRI and NeQuick: features and limitations. Advances in Space Research, 37(5), pp.937-942.
Ezquer, R. G., Adler, N.O., Radicella, S.M., Gonzalez, M .M., and Manza, J . R. (1992): Total electron content obtained from ionogram data alone, Radio Science, **27(**3), 429-434.
Fejer, B. G. and L. Scherliess. 2001. "On the Variability of Equatorial F-Region Vertical Plasma Drifts." 63:893–97.
Huang, X., and Reinisch, B. W. (2001). Vertical electron content from ionograms in real time. *Radio Science*, *36*(2), 335-342.
Huang and Reinisch 1996 Huang, Xueqin and B. W. Reinisch. 1996. "Vertical Electron Density Profiles from the Digisonde Network." 18(6).
Jee, G., Schunk, R.W. and Scherliess, L., 2005. On the sensitivity of total electron content (TEC) to upper atmospheric/ionospheric parameters. Journal of atmospheric and solar-terrestrial physics, 67(11), pp.1040-1052.
Jesus, R De, P R Fagundes, A Coster, O S Bolaji, J H A Sobral, I S Batista, AJ De Abreu, et al. 2016. Effects of the Intense Geomagnetic Storm of September – October 2012 on the Equatorial, Low- and Mid-Latitude F Region in the American and African Sector during the Unusual 24th Solar Cycle." Journal of Atmospheric and Solar-Terrestrial Physics 138–139. Elsevier: 93–105. doi:10.1016/j.jastp.2015.12.015.
Jodogne J.-C., H. Nebdi, and R.Warnan. 2004. Advances in Radio Science GPS TEC and ITEC from Digisonde Data Compared with NeQuick Model. 269–73.

Karia, S.P., and Pathak, K.N.(2011): GPS based Tec measurement for a period Aug 2008-Dec 2009 near the northern crest of India equatorial ionospheric anomaly region. Journal of earth system science, **120**.5, 851-858.

Kenpankho, P., P. Supnithi, and T. Nagatsuma. 2013. ScienceDirect Comparison of Observed TEC Values with IRI-2007 TEC and IRI-2007 TEC with Optional Fo F2 Measurements Predictions at an Equatorial Region, Chumphon, Thailand. Advances in Space Research

Kumar, S., and Singh, A.K. (2009): Variation of ionospheric total electron content in Indian low latitude region of the equatorial anomaly during May 2007–April 2008, Advances in Space Research **43**, 1555–1562.

Langley, R., M. Fedrizzi, E. Paula, M. Santos, and A. Komjathy (2002), Mapping the low latitude ionosphere with GPS, GPS World, 13(2), 41–46.

Leong, S. K. et al. 2014. Assessment of Ionosphere Models at Banting: Performance of IRI-2007, IRI-2012, and NeQuick 2 Models during the Ascending Phase of Solar Cycle 24. Advances in Space Research (2013) http://dx.doi.org/10.1016/j.asr.2014.01.026).

Liu, J. Y., H. F. Tsai, and T. K. Jung (1996b), Total electron content obtained by using the global positioning system, Terr. Atmos. Oceanic Sci., 7, 107.

Mala, S., Bagiya, H. P., Joshi, K. N., Iyer, M., Aggarwal, S., Ravindran, and Pathan, B.M. (2009): TEC variations during low solar activity period (2005–2007) near the equatorial Ionospheric Anomaly Crest region in India, Ann. Geophys., **27,** 1047–1057.

Mannucci, A. J., B. D. Wilson, and C. D. Edwards (1993), A new method for monitoring the Earth's ionospheric total electron content using the GPS global network, paper presented at ION GPS-93, Inst. of Navigation., pp. 1323–1332, Salt Lake City, Utah, 22–24 Sept.

McKinnell, L. A., Opperman, B., and Cilliers, P. J. (2007). GPS TEC and ionosonde TEC over Grahamstown, South Africa: First comparisons. *Advances in Space Research*, *39*(5), 816-820.

McNamara, L.F (1985). The use of total electron content measurements to validate empirical models of the ionosphere. Adv. Space Res. **5** (7), 81– 90.

Migoya Orué, Y. O., S. M. Radicella, P. Coïsson, R. G. Ezquer, and B. Nava. 2008. Comparing TOPEX TEC Measurements with IRI Predictions." Advances in Space Research 42(4):757–62.

Migoya-Orué, Y., Folarin-Olufunmilayo, O., Radicella, S., Alazo-Cuartas, K., and Rabiu, A. B. (2017). Evaluation of NeQuick as a model to characterize the Equatorial Ionization Anomaly over Africa using data ingestion. *Advances in Space Research*, *60*(8), 1732-1738.

Mosert, M, L A McKinnell, M Gender, C Brunini, J Araujo, R G Ezquer, and M Cabrera. 2007. "Variations of F O F 2 and GPS Total Electron Content over the Antarctic Sector," 327–33. doi:10.5047/eps.2011.01.006.

Mosert, M., Gende, M., Brunini, C., Ezquer, R., and Altadill, D. (2007). Comparisons of IRI TEC predictions with GPS and digisonde measurements at the Ebro. *Advances in Space Research*, *39*(5), 841-847.

Nava, B. and S. M. Radicella. 2009. "On the Use of NeQuick Topside Option in IRI-2007." 43:1688–93.

Obrou, O.K., Mene, M.N., Kobea, A.T., and Zaka, K.Z. (2008): Equatorial total electron content (TEC) at low and high solar activity, Advances in Space Research **43**, 1757–1761.

Okoh, D., McKinnell, L.A., Cilliers, P., Okere, B., Okonkwo, C. and Rabiu, B., 2015. IRI-vTEC

versus GPS-vTEC for Nigerian SCINDA GPS stations. Advances in Space Research, 55(8), 1941-1947.

Olatunji, E. O. (1967). The total columnar electron content of the equatorial ionosphere. *Journal of Atmospheric and Terrestrial Physics*, *29*(3), 277-285.

Olawepo, A.O,; Oladipo, O.A; Adeniyi, J.O; and Doherty, P.H (2015). TEC response at two equatorial stations in the African sector to geomagnetic storms. Advances in Space Research 56, 19-27

Olwendo, O. J., P. Baki, P. J. Cilliers, C. Mito, and P. Doherty. 2013. "Comparison of GPS TEC Variations with IRI-2007 TEC Prediction at Equatorial Latitudes during a Low Solar Activity (2009-2011) Phase over the Kenyan Region." Advances in Space Research 52(10).

Olwendo, O. J., P. Baki, P. J. Cilliers, C. Mito, and P. Doherty. 2012. "Comparison of GPS TEC Measurements with IRI-2007 TEC Prediction over the Kenyan Region during the Descending Phase of Solar Cycle 23." Advances in Space Research 49(5):914–21. Retrieved (http://dx.doi.org/10.1016/j.asr.2011.12.007).

Olwendo, O.J., Baki, P., Cilliers, P.J., Mito, C., and Doherty, P. (2012): Comparison of GPS TEC measurements with IRI-2007 TEC prediction over the Kenyan region during the descending phase of solar cycle 23, Advances in Space Research **49**, 914–921.

Rabiu, A. B., A. O. Adewale, R. B. Abdulrahim, and E. O. Oyeyemi. 2014. "ScienceDirect TEC Derived from Some GPS Stations in Nigeria and Comparison with the IRI and NeQuick Models." Advances in Space Research 53(9):1290–1303. Retrieved (http://dx.doi.org/10.1016/j.asr.2014.02.009).

Radicella, S.M., Bilitza, D., Reinisch, B.W., and Adeniyi, J.O., Mosert Gonzalez, M.E., Zolesi, B., Zhang, M.L., Zhang, S. (1998): IRI Task Force Activity At ICTP: Proposed Improvements For The IRI Region Below The F Peak, Adv. Space Res. **22(**6) 731-739.

Rama Rao, P.V.S., Gopi Krishna, S., Niranjan, K., Prasad, D.S.V.V.D. Temporal and spatial variations in TEC using simultaneous measurements from the Indian GPS network of receivers during the low solar activity period of 2004–2005. Ann. Geophys. 24, 3279–3292, 2006b.

Rama Rao, P.V.S., Niranjan, K., Prasad, D.S.V.V.D., Gopi Krishna, S., Uma, G. On the validity of the ionospheric pierce point (IPP) altitude of 350 km in the equatorial and low latitude sector. Ann. Geophys. 24, 2159–2168, 2006a.

Rastogi, R G., and Sharma, R. P. (1971): Ionospheric electron content at Ahmedabad (near the crest of the equatorial anomaly) by using beacon satellite transmissions during half a solar cycle; Planet. Space Sci. **19** 1505–1517.

Rastogi, R.G., Iyer, K.N. and Bhattacharyya, J.C., 1975. Total electron content of the ionosphere over the magnetic equator. Current Science, pp.531-533.

Rawer, K. and Bilitza, D., 1990. International Reference Ionosphere—plasma densities: status 1988. Advances in space research, 10(8), pp.5-14

Rawer, K., Lincoln, J. V., and Conkright, R. O. (1981): International Reference Ionosphere—IRI 79, World Data Center A for Solar-Terrestrial Physics, Report UAG-82, Boulder, Colorado. 52. 223-232.

Reinisch, B.W., Huang, X. Deducing topside profile and total electron content from bottomside ionograms. Adv. Space Res. 27 (1), 23–30, 2001.

Reinisch, B. W. Ã., X. Huang, I. A. Galkin, V. Paznukhov, and A. Kozlov. 2005. “Recent Advances in Real-Time Analysis of Ionograms and Ionospheric Drift Measurements with Digisondes.” 67:1054–62.

Reinisch, B. W., X. Huang, A. Belehaki, and R. Ilma. 2004. “Advances in Radio Science Using Scale Heights Derived from Bottomside Ionograms for Modelling the IRI Topside Profile.” (June 2002):293–97.

Rios, V.H., Medina, C.F. and Alvarez, P., 2007. Comparison between IRI predictions and digisonde measurements at Tucuman. Journal of Atmospheric and Solar-Terrestrial Physics, 69(4-5), pp.569-577.

Skinner, N. J. (1966): Measurements of Total Electron Content Near The Magnetic Equator, Planet. Space Sci. Vol. **14**, Pp. 1123 - 1129.

Scherliess, L., and B. Fejer, Radar and satellite global equatorial F region vertical drift model, J. Geophys. Res., 104,6829-6842,1999.

Sulungu, Emmanuel Daudi, Christian B. S. Uiso, and Patrick Sibanda. 2017. “Comparison of GPS Derived TEC with the TEC Predicted by IRI 2012 Model in the Southern Equatorial Ionization Anomaly Crest within the Eastern Africa Region.” *Advances in Space Research*. Retrieved (http://dx.doi.org/10.1016/j.asr.2017.07.040).

Tariku, Yekoye. 2015. “Patterns of GPS-TEC Variation over Low-Latitude Regions (African Sector) during the Deep Solar Minimum (2008 to 2009) and Solar Maximum (2012 to 2013) Phases.” Earth, Planets, and Space 67 (1). doi:10.1186/s40623-015-0206-2.

Wu C-C, Liou K., Shan, S. J., and Tseng, C. L. (2008): Variation of ionospheric total electron content in Taiwan region of the equatorial anomaly from 1994 to 2003, Advances in Space Research **41**, 611–616.

Yu, Xiao, Chengli Shi, Dun Liu, and Weimin Zhen. 2012. "A Preliminary Study of the NeQuick Model over China Using GPS TEC and Ionosonde Data.” 2012 10th International Symposium on Antennas, Propagation and EM Theory, ISAPE 2012 (36):627–30.

Cherniak and Zakharenkova 2016 Cherniak, Iurii and Irina Zakharenkova. 2016. “NeQuick and IRI-Plas Model Performance on Topside Electron Content Representation: Spaceborne GPS Measurements.” 1–15.

Huang, Xueqin and B. W. Reinisch. 1996. “Vertical Electron Density Profiles from the Digisonde Network.” 18(6).

Zhang, Man Lian, Sandro M. Radicella, Jian Kui Shi, Xiao Wang, and Shun Zhi Wu. 2006. “Comparison among IRI, GPS-IGS and Ionogram-Derived Total Electron Contents.” Advances in Space Research 37(5):972–77.

Zhang, M.I., J.K. Shi, X. Wang and S.M. Radicella (2004), Ionospheric variability at low latitude station: Hainan, China, Advances in Space Science, 34, 1860-1868

8.0 Figures

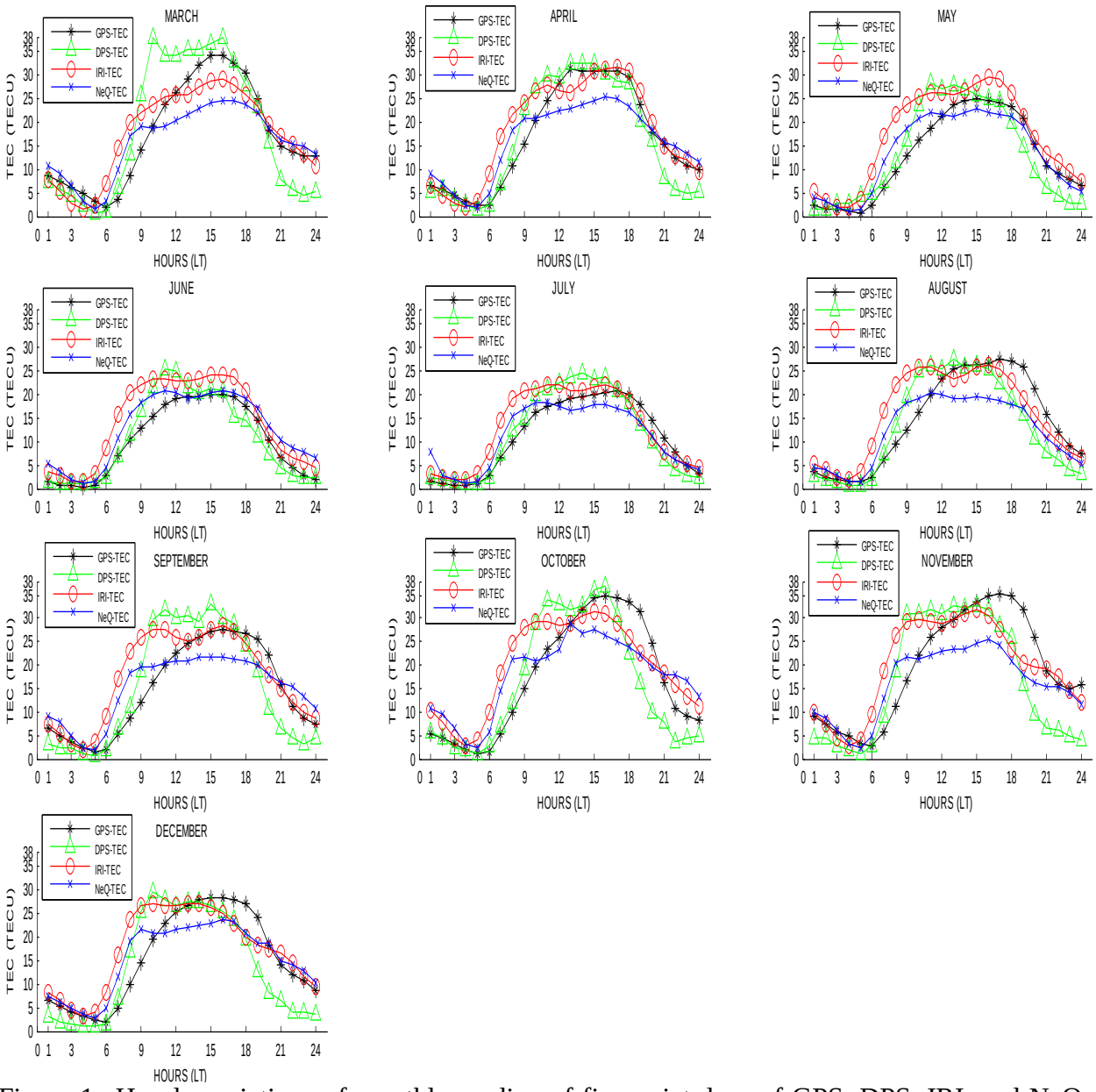

Figure 1a Hourly variations of monthly median of five quiet days of GPS, DPS, IRI, and NeQ-TEC in March-December during quiet period. GPS-TEC is in black line with star symbol, DPS-TEC is in green line with diamond symbol, IRI-TEC is in red line with zero line with star symbol and NeQ-TEC is in blue line with star symbol.

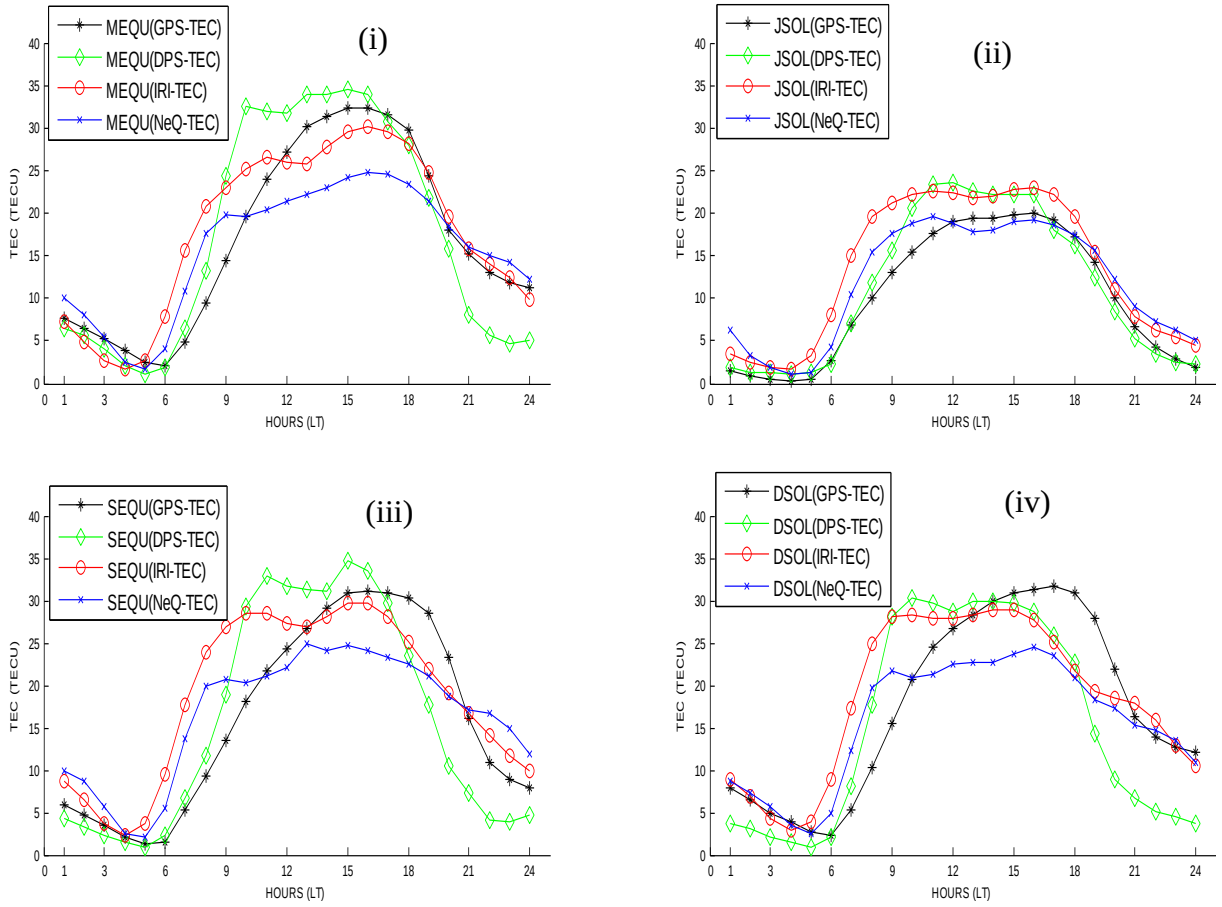

Fig. 1b Seasonal variations of GPS-TEC, DPS-TEC, IRI-TEC and NeQ-TEC for: (i) March Equinox, (ii) June Solstice, (iii) September Equinox, and (iv) December Solstice over Ilorin during quiet periods in 2010. The line colors and symbols are the same as for diurnal variation in Figure 1a for all seasons.

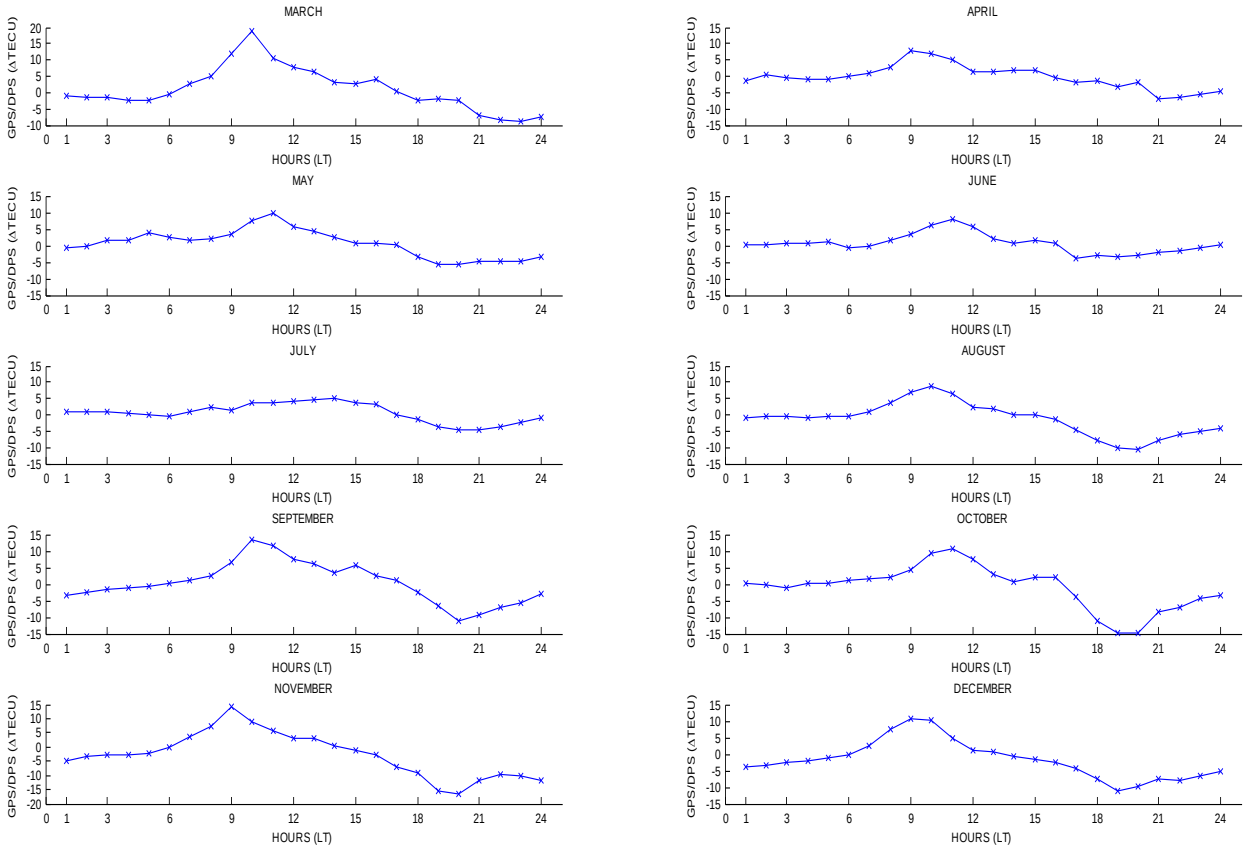

Figure 2a Hourly variations of ΔTEC between the GPS-TEC and DPS-TEC from March - December during quiet period.

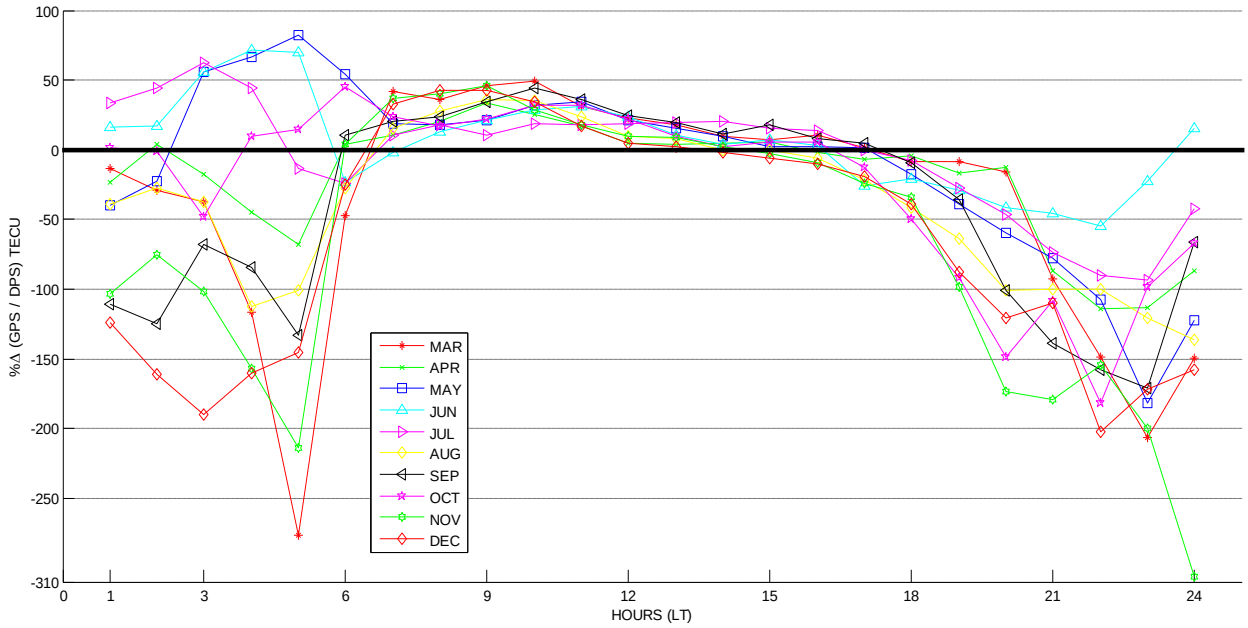

Figure 2b Mass plot of %Δ TEC between the GPS-TEC and DPS-TEC from March - December during quiet period. The legend represents line colors and symbols of each deviation in all months.

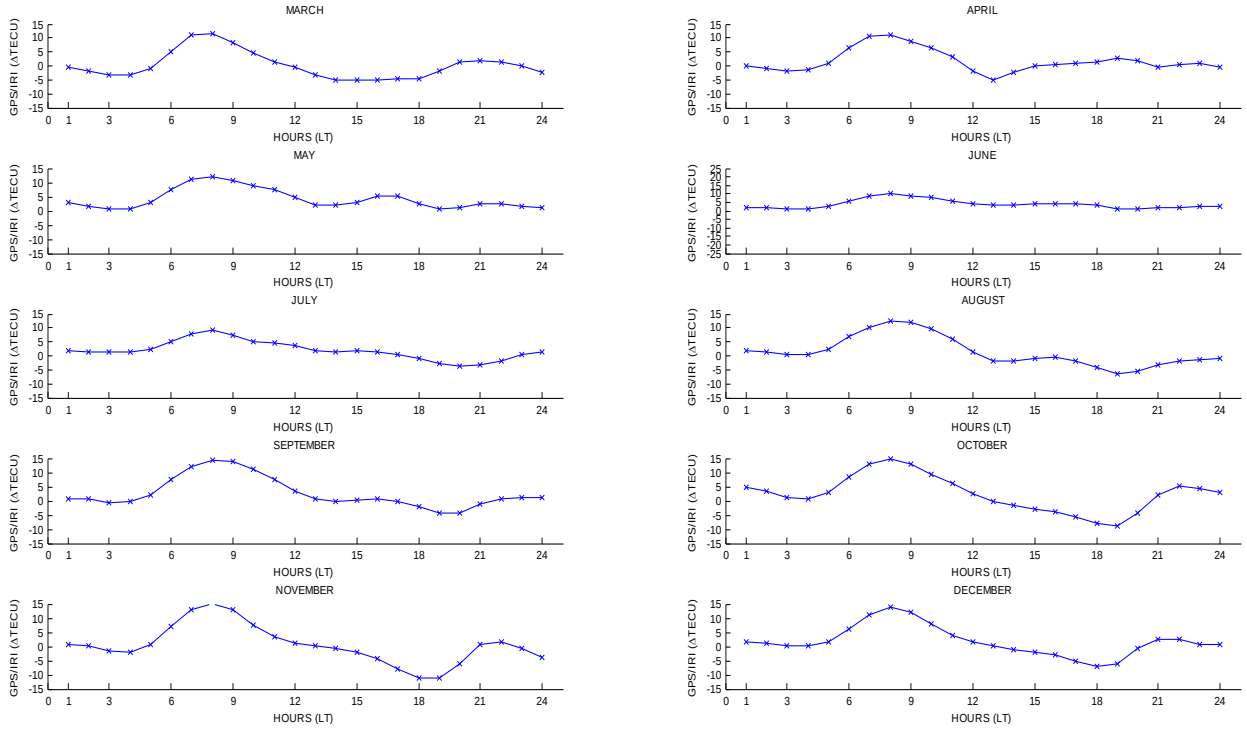

Figure 3a Hourly variations of ΔTEC between the GPS-TEC and IRI-TEC from March - December during quiet period.

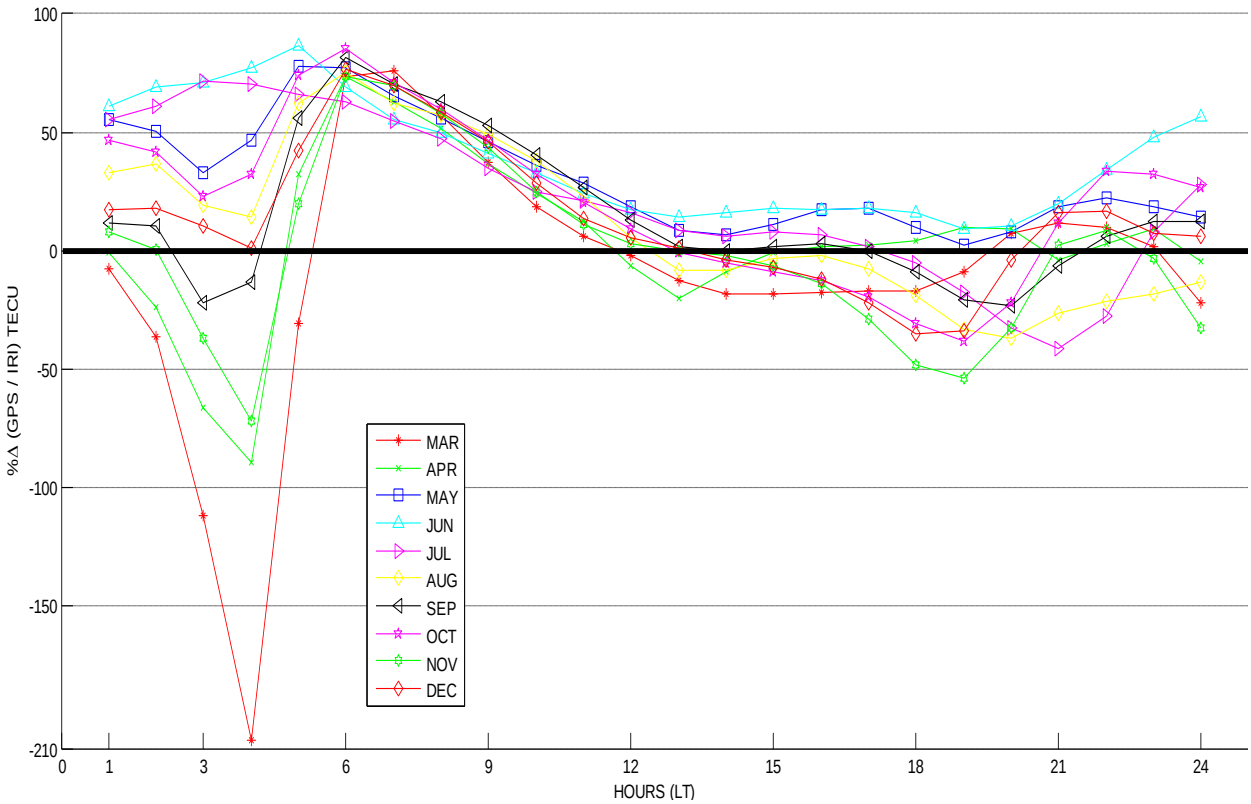

Figure 3b Mass plot of %Δ TEC between the GPS-TEC and IRI-TEC from March to December during quiet period. The line colors and symbols are the same as in Figure 2b

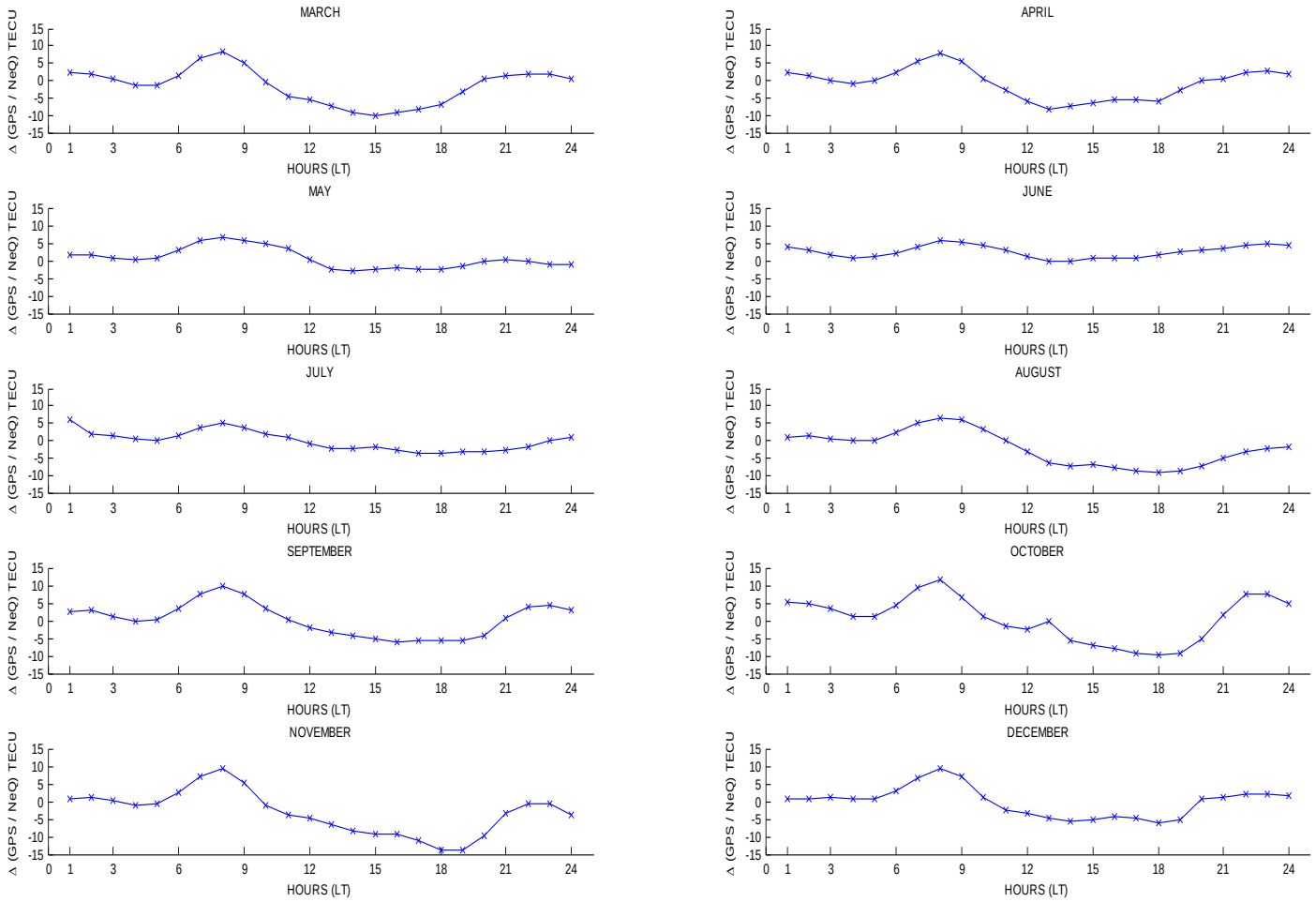

Figure 4a Hourly variations of ΔTEC between the GPS-TEC and NeQ-TEC from March - December during quiet period.

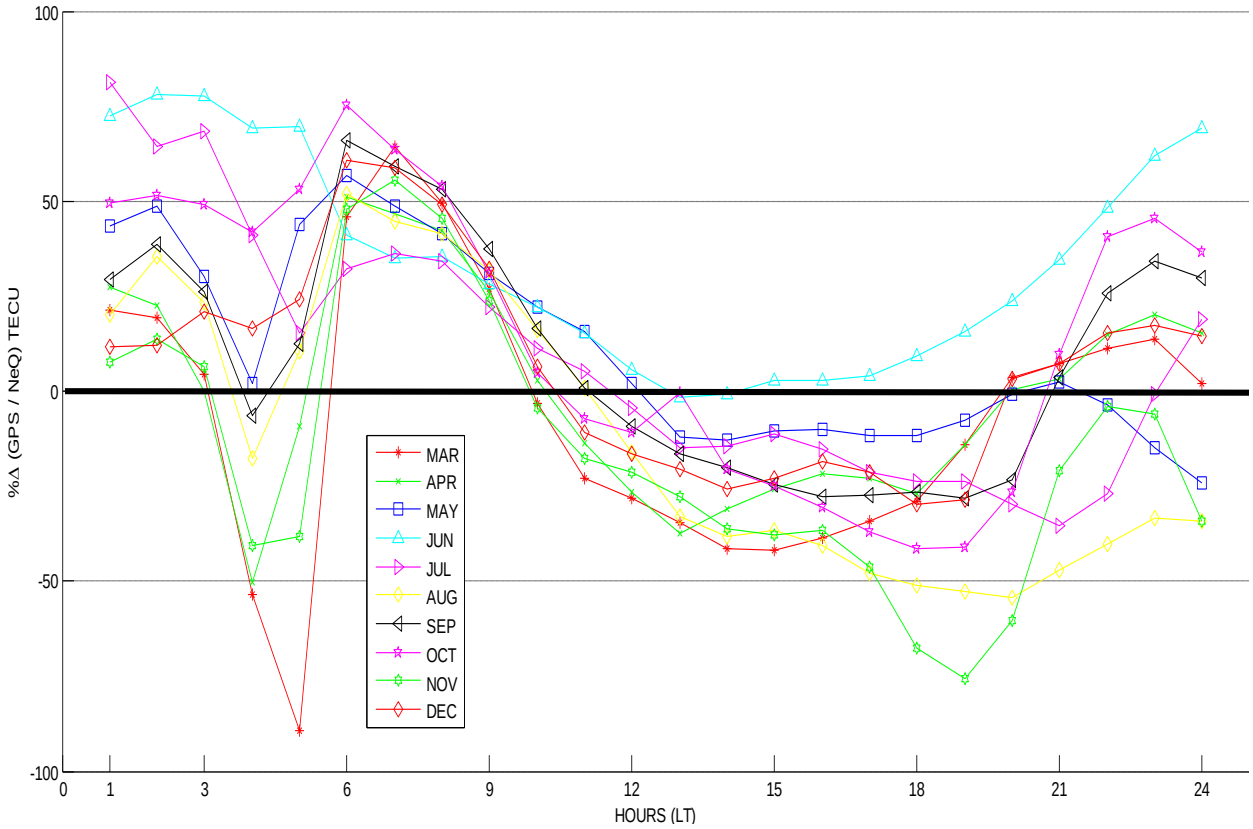

Figure 4b Mass plot of % Δ TEC between the GPS-TEC and NeQ-TEC from March - December during quiet period. The line colors and symbols are the same as in Figure 2b.